ELEVENTH EUROPEAN ROTORCRAFT FORUM

10 — 13 September, 1985 London, England

# ELASTIC FUSELAGE MODES AND HIGHER HARMONIC CONTROL IN THE COUPLED ROTOR/AIRFRAME VIBRATION ANALYSIS

by

S. Hanagud, M. Meyyappa, S. Sarkar, and J. I. Craig
School of Aerospace Engineering
Georgia Institute of Technology
Atlanta, Georgia 30332

# ELASTIC FUSELAGE MODES AND HIGHER HARMONIC CONTROL IN THE COUPLED ROTOR/AIRFRAME VIBRATION ANALYSIS

by

S. Hanagud, M. Meyyappa, S. Sarkar, and J. I. Craig
School of Aerospace Engineering
Georgia Institute of Technology
Atlanta, Georgia 30332 U.S.A.

## ABSTRACT

A coupled rotor/airframe vibration analysis model has been used to study variations in the control vector and vibration levels of the fuselage. The differences between minimization of the hub forces and the acceleration at selected fuselage locations have been discussed. Also the effects of nonideal conditions in the implementation of higher harmonic control and the resulting residual vibration levels in the fuselage have been discussed. The coupled rotor/airframe vibration model is based on the Hsu and Peters rotor model, a finite element fuselage model and impedance matching techniques.

## I. INTRODUCTION

The subject of airframe vibration analysis and the reduction of vibration levels is important in developing designs that provide better occupant comfort, improved visual acuity and prolonged fatigue lives of airframe structures and other equipment. Extensive studies involving dynamic modeling of the fuselage, evaluation of their dynamic characteristics and the needed validation by ground vibration tests are in progress. In many cases, there are discrepancies between the analytical models and test results. Attempts are being done to reconcile these differences by improved modeling techniques and structural dynamic system identification techniques. However, accurate predictions of vibration levels require a knowledge of the exciting forces and other vibration reduction devices. The exciting forces include contributions from the rotor systems and the fixed or nonrotating system. The main rotor system contributions need considerations of the structural dynamics of the blades, the appropriate aerodynamics and the effects of vibration control processes such as the higher harmonic control. This paper is addressed to the problem of vibration predictions in the airframe due to main rotor contributions including the effects of higher harmonic control and their practical implementation.

Practical implementations of higher harmonic control has resulted in incomplete vibration reduction. Some of the unsatisfactory vibration reductions with the classical constant gain control and some adaptive control techniques have been attributed to reasons[1,2] such as nonlinear effects, convergence of the control algorithm to an incorrect minimum, control vectors based on incorrect flight conditions, error sensitivity and other problems such as hardware-software problems. Accurate predictions of air frame vibrations are not possible unless the actual reason for the unsuccessful reduction of vibration levels is incorporated into the vibration analysis. On the bright side of the picture flight test results are now becoming available.[3,4] If a reasonably accurate apriori model is developed for the analysis airframe vibrations that includes higher harmonic control effects, flight test results and system identification techniques can be used to identify and separate the reasons for unsuccessful vibration reductions. Such an identification process will also assist in improving real time control techniques with or without a knowledge base.

Developments and some results of a coupled rotor/airframe vibration model with higher harmonic control are discussed in this paper. Previous attempts at developing such a model has been reported by Sopher Studwell, Cassarino and Kottapalli.[5] In Reference 5, Sopher, Studwell, Cassarino and Kottapalli have developed a coupled rotor/airframe vibration analysis computer program that can predict effects of higher harmonic control on changes in vibration levels. Presented results that use the scale model wind tunnel test data indicate that the model has the capability to adequately predict trends of the variation with the air speed and higher harmonic control inputs. The predicted vibration levels are sensitive to fuselage modal characteristics. The changes in vibration levels due to higher harmonic control were underpredicted and were sensitive to modal characteristics. Also absolute vibration levels with nine fuselage modes are different from measured values but indicated a correct trend.

The approach in this paper is to start with a simple coupled rotar/air frame model that includes higher harmonic effects. The objective is to later generalize the simple model to include additional structural dynamic capabilities, aerodynamic capabilities and control algorithms. By this process it is expected that unimportant parameters and their effects can be eliminated to keep a simple model. A first attempt here is to generalize Hsu and Peters[6] coupled rotor/airframe model to include the effects of higher harmonic control and study the effects of some of the postulated reasons for unsuccessful reductions.

## II. BACK GROUND

In the past few years, many active vibration control techniques[1-4, 7-17] have been proposed to overcome the possible weight penalties and lack of flexibility of passive vibration control options. This paper is concerned with one of the active control techniques that uses the blade pitch motions at

higher harmonics in the rotating frame. The potential benefits of the higher harmonic control techniques have already been demonstrated.[6-12] As is well known, basic principles of this control technique consists of superposing higher harmonics on the 0/rev and 1/rev blade cyclic pitch to achieve a reduction of vibration levels at selected fuselage locations. In practical applications, however, vibratory hub loads are detected at b/rev for a 'b' bladed rotor system and a control algorithm is then used to determine the amplitude and phase of the rotor higher harmonic inputs to reduce the vibratory hub loads. It is then expected that a reduction of the vibratory hub loads and moments results in a reduction of vibration levels of the airframe. It is usually assumed that, for a 'b' bladed rotor system, the significant airframe excitation frequencies is at b/rev even though the airframe excitation frequencies occur at other integral multiples of b/rev because of the larger contribution of lower harmonics. Other purposes of higher harmonic control has included objectives such as reduction of blade stresses, etc.

It has also been noted that, for best results, amplitudes and phases of the needed higher harmonics vary considerably for different flight conditions and different choice of locations where reductions of vibration levels are sought. As a consequence, a significant amount of recent research work has focussed on inflight adjustments, uses of recursive estimation procedures and adaptive control techniques to achieve optimum changes in vibration levels for different fight conditions.

## III. COUPLED ROTOR/AIRFRAME MODEL WITH HHC

As discussed earlier, the approach is to start with a simple model and later progressively add additional complexities. Some of the reasons for such an approach is to be able to answer the following questions.

(1) Under what conditions is the rotor/airframe coupling important in predicting high harmonic control effects on airframe vibrations in practice?

(2) If the airframe coupling is important what type of airframe structural dynamic model is adequate? How simple a model will suffice to yield the desired results? How many and what types of degrees of freedom are important? Are simple assumed mode models such as beam type of fuselage models are accurate enough to predict the desired higher harmonic effects and changes in vibration levels including the reasons for unsuccessful reductions and adaptive control?

(3) Does a simple rotor system model with quasi steady aerodynamic yield the desired results? If not how complicated should the model be? What type of aerodynamics is necessary to predict the desired effects?

The coupled rotor-airframe vibration model that is used is based on the work of HSU and Peters.[6, 18] This model is based on an impedance matching method and thus provides the simplicity of performing separate calculations for the rotor system and the fuselage. The separate derivations are followed by procedures involving matching of appropriate forces and moments. In such an analysis calculations are needed only for a single blade. Results for multiblade rotor system are obtained by appropriate transformations.

In developing the model, Hsu and Peters' have assumed a uniform blade that is quantitatively described by modal coordinates $q_i$ in "flapping only" conditions. As discussed in the previous section, this assumption has been retained in the present analysis to maintain simplicity and study the effects of flapping motion of the rotor and airframe combination on higher harmonic control. Natural extensions of the present analysis is to consider "flap-lag" condition and "flap-lag-torsion" conditions. Reverse flow effects have been included.

There are some differences between Hsu-Peters' model and the model used in this paper. In the present analysis there are two options for the fuselage analysis. A first option is to use a model, similar to that of Hsu and Peters, that is based on the assumption of assumed modes. A second option is to use a model that is based on a finite element approximation. The purpose of the finite element model is to be able to consider larger degrees of freedom in the fuselage and local changes of stiffnesses.

Quantitatively, the coupled rotor airframe model can be explained with reference to Figures 1 and 2. The deformation of the rotor blade

$$w(x, t) = \sum_{i=1}^{N} \phi_i(x)\, q_i(t) \qquad -(3.1)$$

where $\phi_i(x)$ are the assumed modes and $q_i(t)$ are the generalized coordinates. Then, for the rotor blade the dynamic equation are

$$\underset{\sim}{M}_R \ddot{\underline{q}} + \underset{\sim}{D}_c \dot{\underline{q}} + (\underset{\sim}{D}_k + \underset{\sim}{P} + \underset{\sim}{K})\underline{q} = \underset{\sim}{D}_v \underline{\theta} + \underset{\sim}{D}_Y \underline{Y} \qquad -(3.2)$$

where $\underline{q}$ is a vector of generalized coordinates.

$$\underline{q}^T = \{ q_1, \ldots, q_N \} \qquad -(3.3)$$

The vector $\underline{\theta}$ is a 10x1 vector

$$\underline{\theta}^T = \{ \theta_0, \theta_1^c, \theta_1^s, \theta_3^c, \theta_3^s, \theta_4^c, \theta_4^s, \theta_5^c, \theta_5^s \} \qquad -(3.4)$$

and $\underline{Y}$ is the vector of forcing terms due to hub motions

$$\underline{Y}^T = \{ \dot{z}_h, \dot{\alpha}_m, \dot{\alpha}_\ell, \ddot{z}_h, \ddot{\alpha}_m, \ddot{\alpha}_\ell \}$$

Other matrices in equation (2-2) are the mass matrix $\underset{\sim}{M}_R$, stiffness matrix $\underset{\sim}{K}_R$, aerodynamic damping matrix $\underset{\sim}{D}_C$, aerodynamic contribution to the stiffness matrix $\underset{\sim}{D}_K$ and the contribution of centrifugal forces to the stiffness matrix $\underset{\sim}{P}$. Parts of the forcing matrix $\underset{\sim}{D}_V$ is due to control variable and $\underset{\sim}{D}_V$ is due to the hub motion. Techniques and equations for determining all these matrices are the same as those discussed in references 1 and 4 with the exception that $D_V$ is different because of the additional higher harmonic terms in control variables and reversed flow effects.

The fuselage model is described by the following equation

$$\underset{\sim}{M}_f \ddot{\underline{W}}_f + \underset{\sim}{C}_f \dot{\underline{W}}_f + \underset{\sim}{K}_f \underline{W}_f = \underline{F} \qquad -(3.5)$$

The quantity $W_f$ is a vector of dimension $N_f$ corresponding to the degree of freedom selected for the fuselage. The vector $W_f$ and the forcing vector $\{F\}$ are partitioned as follows:

$$\underline{W}_f = \begin{Bmatrix} W_{fh} \\ W_{ff} \end{Bmatrix} \quad , \quad \underline{F} = \begin{Bmatrix} F_h \\ F_f \end{Bmatrix} \qquad -(3.6)$$

The vector $W_{fh}$ and $F_h$ correspond to the node at the hub. In the coupled model these displacements and forces are matched with the corresponding displacements and forces of the rotor contributions at the same node. These other quantities are as follows:

$F_f$ = vector of forces applied allocation other than the hub

$F$ = vector of forces applies all fuselage nodes

$W_f$ = vector of displacements at all fuselage nodes

$W_{ff}$ = vector of displacements at all nodes other than the hub

For a harmonic excitation

$$W_f = H_f F \qquad -(3.7)$$

where $H_f$ is fuselage frequency response matrix that can be obtained from (3.5). In partitioned form

$$\begin{Bmatrix} W_{fh} \\ W_{ff} \end{Bmatrix} = \begin{bmatrix} H_{f1} & H_{f2} \\ H_{f3} & H_{f4} \end{bmatrix} \begin{Bmatrix} F_h \\ F_f \end{Bmatrix} \qquad -(3.8)$$

When forces are applied only at the hub, the hub displacements can be expressed as

$$W_{fh} = H_{f1} \; F_h \qquad - (3.9)$$

If the excitations at the hub consist of sums of sines and cosines, i.e.,

$$\{F_h\} = \{F_h{}^c\} \cos \omega t + \{F_h{}^s\} \sin \omega t \qquad - (3.10)$$

The hub displacements become

$$\begin{Bmatrix} W_{fh}^c \\ W_{fh}^s \end{Bmatrix} = \begin{bmatrix} H_{f1}^R & H_{f1}^I \\ -H_{f1}^I & H_{f1}^R \end{bmatrix} \begin{Bmatrix} F_h^c \\ F_h^s \end{Bmatrix} \qquad - (3.11)$$

where $W_{fh}^c$ = vector of amplitudes of cosine response

$W_{fh}^s$ = vector of amplitude of sine response

$H_{f1}^R$, $H_{f1}^I$ = real and imaginary parts of $H_{f1}$

The hub forces and displacements are defined as follows:

$$\underline{P}^T = \{V^c, M_m^c, M_\ell^c, V^s, M_m^s, M_\ell^s\} = \{F_h^c, F_h^s\} \qquad - (3.12)$$

$$\underline{Z}^T = \{Z_h^c, \alpha_m^c, \alpha_\ell^c, Z_h^s, \alpha_m^s, \alpha_\ell^s\} = \{W_{fh}^c, W_{fh}^s\} \qquad - (3.13)$$

Then

$$\underline{Z} = \underset{\sim}{H}_{fh} \, \underline{P} \qquad - (3.14)$$

where

$$\underset{\sim}{H}_{fh} = \begin{bmatrix} H_{f_1}^R & H_{f1}^I \\ -H_{f1}^I & H_{f1}^R \end{bmatrix} \qquad - (3.15)$$

## IV. METHOD OF SOLUTION

The equations are solved by a harmonic balance method by expanding the generalized coordinates in harmonics and equating the coefficients of the corresponding harmonics. For a four bladed rotor system, appropriate third, fourth and fifth harmonics are used.

In particular

$$q_i = q_{i0} + \sum_{n=1}^{7} \left( q_i^{nc} \cos n\Omega t + q_i^{ns} \sin n\Omega t \right) \quad -(4.1)$$

$$Z_h = Z_h^c \cos 4\Omega t + Z_h^s \sin 4\Omega t \quad -(4.2)$$

$$\alpha_m = \alpha_m^c \cos 4\Omega t + \alpha_m^s \sin 4\Omega t \quad -(4.3)$$

$$\alpha_\ell = \alpha_\ell^c \cos 4\Omega t + \alpha_\ell^s \sin 4\Omega t \quad -(4.4)$$

By defining

$$\underline{\bar{q}}^T = \left\{ q_{10}\ q_1^{1c}\ q_1^{2c} \ldots q_1^{7c}\ q_1^{1s} \ldots q_1^{7s} \ldots q_{N0}\ q_N^{1c} \ldots\ q_N^{7s} \right\} \quad -(4.5)$$

$\bar{q}$ can be expressed as

$$\underline{\bar{q}} = \underset{\sim}{Q}' \underline{\theta} + \underset{\sim}{H}' \underline{Z} \quad -(4.6)$$

and from (4-6) hub forces P of (3-12) can be written as

$$\underline{P} = \underset{\sim}{Q}\, \underline{\theta} + \underset{\sim}{H}\, \underline{Z} \quad -(4.7)$$

The matrices Q and H are obtained from (4-6).

From (3.16) and (4.3)

$$\underline{P} = \left( \underset{\sim}{I} - \underset{\sim}{H}\, \underset{\sim}{H}_{fh} \right)^{-1} \underset{\sim}{Q}\, \underline{\theta} = \underset{\sim}{\bar{H}}\, \underline{\theta} \quad (4.8)$$

and

$$\underline{Z}_f = \begin{Bmatrix} W_f^c \\ W_f^s \end{Bmatrix} = \begin{bmatrix} H_f^R & H_f^I \\ -H_f^I & H_f^R \end{bmatrix} \begin{Bmatrix} F_h^c \\ 0 \\ F_h^s \\ 0 \end{Bmatrix} \qquad -(4.9)$$

$$\underline{Z}_f = \underline{\underline{H}}\ \underline{\theta} \qquad -(4.9a)$$

Trim conditions are determined by the usual procedures that ensure a balance of forces and moments at the fuselage c.g. The higher harmonic control vector is defined as follows.

$$\underline{\theta}_{HHC}^T = \left\{ \theta_3^c, \theta_3^s, \theta_4^c, \theta_4^s, \theta_5^c, \theta_5^s \right\} \qquad -(4.10)$$

Optimum values for the control variables are determined by either minimizing the forces or the displacements (or acceleration). When the forces are minimized, the control vector is chosen to optimize the following objective function.

$$J = \underline{P}^T \underline{\underline{W}}_P \underline{P} + \underline{\theta}_{HHC}^T \underline{\underline{W}}_\theta \underline{\theta}_{HHC} \qquad -(4.11)$$

where $W_p$ and $W_\theta$ are diagonal weighting matrices and the second term is included to reduce the control amplitudes. The vector of hub forces P can be expressed as

$$\underline{P} = \underline{P}_0 + \underline{\underline{\bar{H}}}_{HHC}\ \underline{\theta}_{HHC} \qquad -(4.12)$$

where $P_0$ = hub forces at trim when $\theta_{HHC} = 0$

$\bar{H}_{HHC}$ = part of $\bar{H}$ that corresponds to $\theta_{HHC}$

Minimizing J with respect to $\theta_{HHC}$ leads to

$$\theta_f^* = -\left[ \underline{\underline{\bar{H}}}_{HHC}^T \underline{\underline{W}}_P\ \underline{\underline{\bar{H}}}_{HHC} + \underline{\underline{W}}_\theta \right]^{-1} \underline{\underline{\bar{H}}}_{HHC}^T \underline{\underline{W}}_P \underline{P}_0 \qquad -(4.13)$$

where $\theta_f^*$ is the optimum control vector.

When displacements (or acceleration) are considered instead of the hub forces, the controls are evaluated by minimizing

$$J = \underline{Z}_f^T \underline{\underline{W}}_Z \underline{Z}_f + \underline{\theta}_{HHC}^T \underline{\underline{W}}_\theta \underline{\theta}_{HHC} \qquad -(4.14)$$

which results in

$$\theta_a^* = -\left[\bar{\bar{H}}_{HHC}^T W_Z \bar{\bar{H}}_{HHC} + W_\theta\right]^{-1} \bar{\bar{H}}_{HHC}^T W_Z Z_o^f \quad -(4.15)$$

where $Z_f = Z_o^f + \bar{\bar{H}}_{HHC}\ \theta_{HHC}$

$Z_o^f$ = displacements (or accelerations) at trim when $\theta_{HHC} = 0$

$\bar{\bar{H}}_{HHC}$ = part of that corresponds to $\theta_{HHC}$

and $\theta_a^*$ = optimum control when displacements (or acceleration) are minimized

## NUMERICAL RESULTS AND DISCUSSIONS

Discussions in this paper are directed toward the possibility of developing a capability to predict airframe vibration levels and their changes with higher harmonic control. In order to develop such a capability, it is necessary to determine how a particular higher harmonic control algorithm and its practical implementation will change the fuselage exciting forces and eventually fuselage displacements, velocites and accelerations. If higher harmonic control is implemented under ideal conditions such as linearity, error free estimation of flight conditions, use of the exact instantaneous flight conditions to calculate the higher harmonic corrections, convergence to the correct minimum and absence of any hardware - software problems the higher harmonic control will reduce b/rev hub forces to zero. However, this is not the case in practice. It is necessary to consider these nonideal conditions. Both ideal and some nonideal conditions are discussed in this paper.

First, the control parameters are discussed under ideal conditions by selecting a rotor system and two models for the fuselage. The coupled rotor/airframe model discussed in the previous section has been used. The discussions are concerned with the uncontrolled forces, uncontrolled accelerations, the control parameters that are necessary when the hub forces or minimized and the necessary parameters when the accelerations in the fuselage at a selected location are minimized. Next, the possibility of selecting an incorrect flight condition or convergence to a false minimum is discussed. The resulting vibration levels in the fuselage have been calculated. Then, the following question has been asked. If these vibration levels have been measured in a flight test is it possible to use their measurements and structural dynamic system identification techniques to determine the actual flight condition used in the control algorithm, and the resulting hub forces that were acting on the fuselage?

The selected rotor model had properties described in Table I. The properties used for the finite element model for the fuselage are shown in Table II. The assumed mode model for the fuselage has (Table III)nine degrees

of freedom. The model had one each rigid body degree of freedom and two elastic modes in plunge, pitch and roll degrees of freedom. Some of the calculations are only with six degrees of freedoms. The finite element model had eleven nodes and thirty three degrees of freedom. (Figure 3)

In Figure 4 variations of trim conditions, i.e., $\theta_0$, $\theta_1^C$, $\theta_1^S$, and $\lambda$ with the advance ratio $\mu$ has been illustrated. Figures without subscript refer to the finite element model fuselage and the figures with subscript a refer to the assumed mode model for the fuselage. The 4/rev uncontrolled $C_T$ and its variations with the advance ratio are illustrated in Figure 5. Similarly, the 4/rev uncontrolled pitching moment coefficient $C_M$ variations with the advance ratio are illustrated in Figure 6. In Figure 7, the uncontrolled accelerations at the node representing the pilot seat has been illustrated. The higher harmonic control vector, i.e., $\theta_3$, $\theta_4$, and $\theta_5$ that are necessary to control the hub forces or accelerations as functions of the advance ratio $\mu$ are illustrated in Figures 8, 9, and 10. The values of $\theta_3$, $\theta_4$, and $\theta_5$ in these figures represent their magnitude. Two curves in each of the Figures 8, 9, 10 represent two different conditions for the evaluation of the higher harmonic control vector. One curve represents the values of the control parameter where hub forces are minimized. The second curve represents the values of the parameters where the accelerations at the node representing the pilot seat are minimized. The weighting factors for the minimization of the hub forces and moments constitute a diagonal matrix with values of $R^2$, 1, and 1. The corresponding weighting matrix for the minimization of accelerations at the node representing the pilot seat is also a diagonal matrix with weights 10, 1, and 1. The value of 10 has been assigned to the vertical acceleration. As can be seen from the figures, even under ideal conditions, the values of the control parameters are different depending up on which quantity is minimized and the weights chosen for different variables. If a limit on the values of the control parameters such as $0.2^0$ or $0.5^0$ are imposed there will be residual of the uncontrolled forces or moments or accelerations for some advance ratios. BAR charts for the hub shear forces and hub bending moments are illustrated in Figures 11 and 12. All harmonics before and after control are illustrated for a selected advance ratio.

Next set of figures are used to illustrate some of the preliminary studies of nonideal conditions. All variations of nonideal conditions have not been studied in this paper. In Figure 13, some of the possible nonideal conditions have been illustrated. Some of these include (a) an assumption of linearity when the actual behavior is nonlinear, (b) incorrect flight conditions used in the estimation of control parameters, (c) convergence to a false minimum, (d) random errors introduced as the control parameters are transferred from the software of the control algorithm to the hardware that implements these control variables. In order to illustrate, two particular conditions involving the convergence of the algorithm to a false minimum and changes in the flight conditions are considered. In order to illustrate changes in the flight conditions advance ratio change from $\mu_1$ to $\mu_2$ in a time duration 't' seconds has been considered. It is assumed that flight conditions have been estimated at specific time values $t_1$ has been used to detect and calculate the control

variables. By the time the changes are computed and implemented via hardware the flight conditions correspond to an advance ratio at $t_1 + t$. In Figure 13 the variations of the advance ratio, $t_1$ and $t$ have been illustrated. In Figure 14, accelerations at a fuselage node because of these nonideal conditions have been illustrated. In Figure 15 use of incorrect flight condition and its effect on controlled accelerations are illustrated. In a practical situation, if these accelerations or some other quantities have been measured and the cause of this particular nonideal condition is not known the following question can be asked. Is it possible to use system identification techniques to determine these conditions? In general is it possible to distinguish between the various causes resulting in an incomplete reduction of vibration levels due to HHC. In Figure 16 accelerations at the node representing pilot seat due to the convergence to a false minimum near a $\mu$ has been illustrated for a selected advance ratio.

In general

$$\underline{Z}_f = \begin{bmatrix} \underline{\underline{H}}_T & \underline{\underline{H}}_{HHC} \end{bmatrix} \begin{Bmatrix} \underline{\theta}_T \\ \underline{\theta}_{HHC} \end{Bmatrix}$$

If $\theta_{HHC}$ is not the correct value corresponding to the trim condition because of an error in the control algorithm $\theta_{HHC} = \theta_C$. Then

$$\underline{Z}_f = \begin{bmatrix} \underline{\underline{H}}_T & \underline{\underline{H}}_{HHC} \end{bmatrix} \begin{Bmatrix} \underline{\theta}_T \\ \underline{\theta}_c \end{Bmatrix}$$

In a very simple identification problem if $\underline{z}_f$ is measured at selected fuselage locations can we find $\theta_c$.

## CONCLUSIONS

The higher harmonic control vectors and their effects on the vibration levels at selected fuselage locations have been studied by using a simple coupled rotor/airframe model. Considerations have been given to different available options such as the minimization of the hub forces and minimization of accelerations in the fuselage. Some effects in the possible practical implementation of HHC have been discussed. Possibilities of identification of the actual HHC input has been discussed. Additional work with (a) more accurate aerodynamical considerations (b) additional degrees of freedom in rotor and fuselage and (c) identification techniques should yield practical insight to the problem.

Acknowledgement: Author gratefully acknowledge support for this work from U.S. Army Research Contract DAAG-29-82-K-0094.

## REFERENCES


1. Moulasis, J.A., "The Importance of Nonlinearity on the Higher Harmonic Control of Helicopter Vibrations," 39th AHS Annual Forum, 1983.

2. Chopra, I., and J. McCloud, "A Numerical Simulation Study of Open-loop, Closed-loop and Adaptive Multicyclic Control Systems," J. American Helicopter Society, p. 63, 1983.

3. Johnson, W. "Recent Developments in the Dynamics of Advanced Rotor Systems," Proc. AGARD Conference on Flight Mechanics, Ed. Co. Reichert, 1984.

4. Wood, E.R., R.W. Powers, J.H. Cline, and C.E. Hammond, "On Developing and Flight Testing a Higher Harmonic Control System," A.H.S. Forum, 1983.

5. Sopher, R., R.E. Studwell, S. Cassarino, and S.B.R. Kottapalli, "Coupled Rotor/Airframe Vibration Analysis," NASA CR 3582, 1982.

6. Hsu, T.K., and D.A. Peters, "Coupled Rotor/Airframe Vibration Analysis by a Combined Harmonic Balance, Impedance Matching Method," J. American Helicopter Society, 1982.

7. Ham, N.D., "Helicopter Individual Blade Control and Applications," Annual National Forum, A.H.S., 1983.

8. Kretz, M., "Research on Multicycle and Active Control of Rotor Wings," Vertica, Vol. 1, No. 2, 1976.

9. Gupta, R., and R.W. Duvall, "A New Approach to Active Control of Rotorcraft Vibration," J. Guidance and Control, 5, 1982.

10. Jacob, H.G., & G. Lehman, "Optimization of Blade Pitch Angle for Higher Harmonic Control," Vertical, 7, 1983.

11. Moulasis, J.A., C.E. Hammond, and J. Cline, "A Unified Approach to the Optimal Design of Adaptive and Gain Scheduled Controllers to Achieve Minimum Helicopter Rotor Vibration," J. American Helicopter Society, p. 9-18, 1981.

12. Wood, E.R., "R.W. Powers and C.E. Hammond, "On Methods for Application of Harmonic Control," Vertica, Vol. 4, p. 43-60, 1980.

13. R.J. London, G.A. Watts, and G.J. Sissingh, "Experimental Hingeless Rotor Characteristics at Low Advance Ratio with Thrust," NASA CR-114684, December 1973.

14. G.J. Sissingh and R.E. Donham, "Hingeless Rotor Theory and Experiment on Vibration Reduction by Periodic Variation of Conventional Controls," Rotorcraft Dynamics, NASA SP-352, February 1974.

15. F.J. McHugh and J. Shaw, Jr., "Benefits of Higher-Harmonic Blade Pitch: Vibration Reduction, Blade-load Reduction and Performance Improvement," Proceedings of the American Society Helicopter Mideast Region Symposium on Rotor Technology, August 1976.

16. F.J. McHugh and J. Shaw, Jr., "Helicopter Vibration Reduction with Higher Harmonic Blade Pitch," Proceedings of the Third European Rotorcraft and Powered-Lift Aircraft Forum, September (1977).

17. C.E. Hammond, "Helicopter Vibration Reduction Via Higher Harmonic Control, Structures Laboratory," U.S. Army Research and Technology Laboratories, Proceedings of the Rotorcraft Vibration Workshop, NASA Ames Research Center, February 1978.

18. Peters, D.A., and R.A. Ormiston, "Flapping Response Characteristics of a Hingeless Rotor Blades by a Generalized Harmonic Balance Method," NASA TN D-7856, 1975.

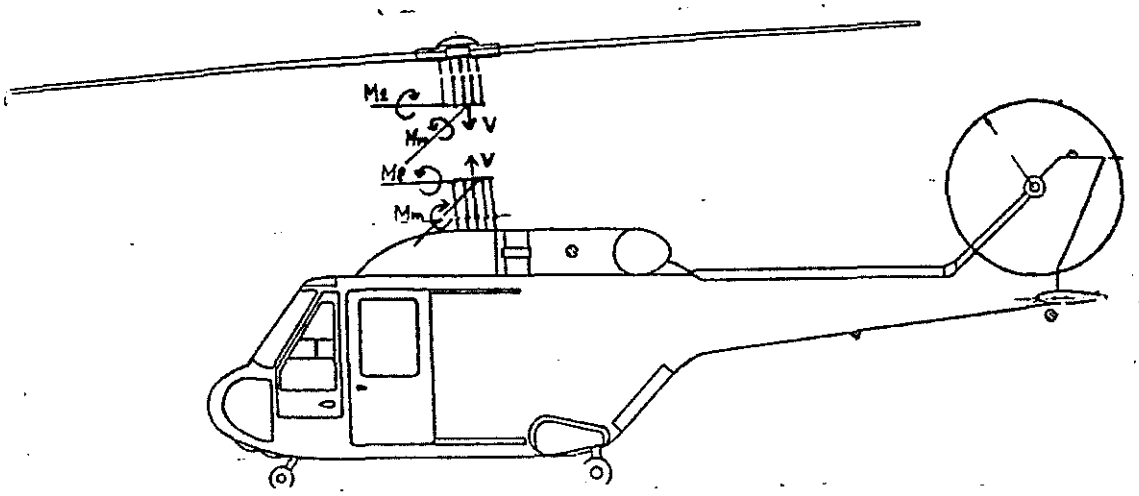


Figure 1 Coupled Rotor/Airframe Model

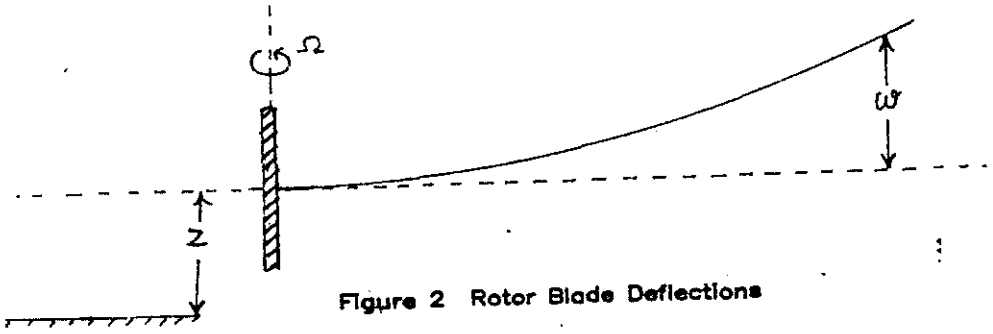


Figure 2 Rotor Blade Deflections

Table I Rotor Properties

| Description | Symbol | Value |
|---|---|---|
| No. of blades | b | 4 |
| Radius | R | 20.8 ft |
| Chord | c | 1.56 ft |
| Mass/Unit Length | m | 0.203 slug/ft |
| Flap Bending Stiffness | E I | $3.128 \times 10^6$ lb–ft$^2$ |
| Lift Curve Slope | a | 5.73 |
| Lock Number | $\gamma$ | 6.53 |
| Rotor speed | $\Omega$ | 33.62 rad/sec |
| First Nonrotating Freq. | $\omega$ | 10.08 rad/sec |
| Density of Air | $\rho$ | .002378 slug/ft$^3$ |
| Solidity | $\sigma$ | 0.095 |

Table IIa Fuselage Mass and Stiffness Properties

| Element No. | Mass/Length slugs/ft | Mass Moment/Length ($\times 10^{-2}$) slugs−ft | Bending Stiffness ($\times 10^{7}$) lbs−ft$^2$ | Torsional Stiffness ($\times 10^{7}$) lbs−ft$^2$ |
|---|---|---|---|---|
| 1 | 1.57 | 8.38 | 1.15 | .86 |
| 2 | 5.76 | 20.94 | 2.88 | 2.16 |
| 3 | 5.76 | 20.94 | 2.88 | 2.16 |
| 4 | 12.56 | 38.74 | 5.33 | 4.00 |
| 5 | 12.56 | 38.74 | 5.33 | 4.00 |
| 6 | 3.14 | 15.70 | 2.16 | 1.62 |
| 7 | .52 | 9.42 | 1.30 | .97 |
| 8 | .52 | 5.23 | .72 | .54 |
| 9 | .42 | 4.19 | .58 | .43 |
| 10 | .42 | 2.09 | .29 | .22 |

( 2% Proportional viscous damping is assumed )

Table IIb Fuselage Concentrated Properties

| Node No. | Mass (slugs) | Rotary Inertia (slugs−ft$^2$) | |
|---|---|---|---|
| | | Pitch | Roll |
| 1 | – | – | 10.0 |
| 2 | – | – | 60.0 |
| 3 | – | – | 100.0 |
| 4 | – | – | 225.0 |
| 5 | 23.4 | 842.4 | 1100.0 |
| 6 | – | – | 225.0 |
| 7 | – | – | 16.0 |
| 8 | – | – | 3.2 |
| 9 | – | – | 2.0 |
| 10 | – | – | 1.0 |
| 11 | – | – | 1.0 |

Table IIc Natural Frequencies of the Fuselage Model

| Mode No. | Frequency (Hz) | Type |
|---|---|---|
| 4* | 8.37 | First vertical bending |
| 5 | 17.40 | Second vertical bending |
| 6 | 21.64 | First torsion |
| 7 | 34.17 | Third Vertical Bending |
| 8 | 34.25 | Second torsion |

* First three modes are rigid body modes

Table III Fuselage Properties ( Nondimensional )

| Description | Symbol | Value |
|---|---|---|
| Unconstrained bending frequency | $\omega_{fv}$ | 1.53 |
| Unconstrained pitching frequency | $\omega_{fl}$ | 3.04 |
| Unconstrained rolling frequency | $\omega_{fm}$ | 2.57 |
| Radius of gyration in pitch | $r_{gm}$ | 0.37 |
| Radius of gyration in roll | $r_{gl}$ | 0.14 |

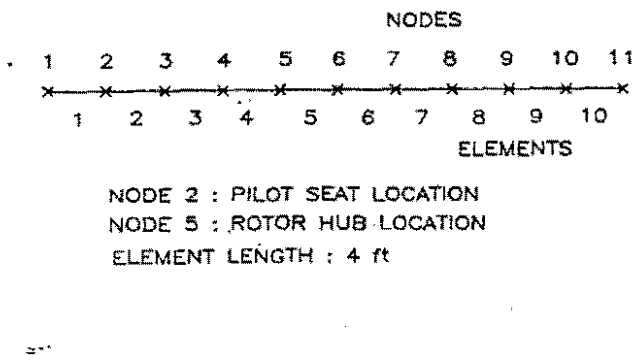


Figure 3 Beam Model for the Fuselage

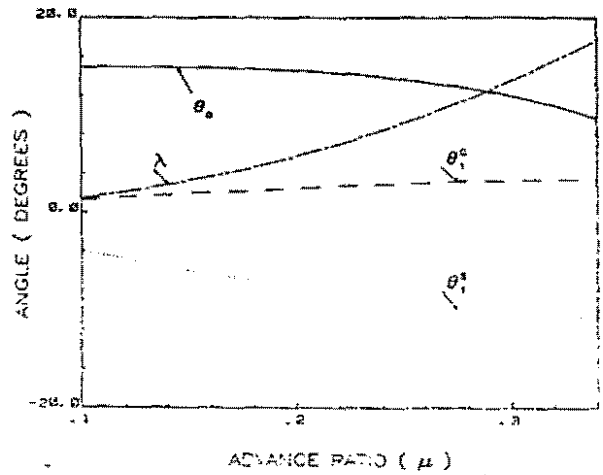


Figure 4 Variation of Trim Conditions with Advance Ratio

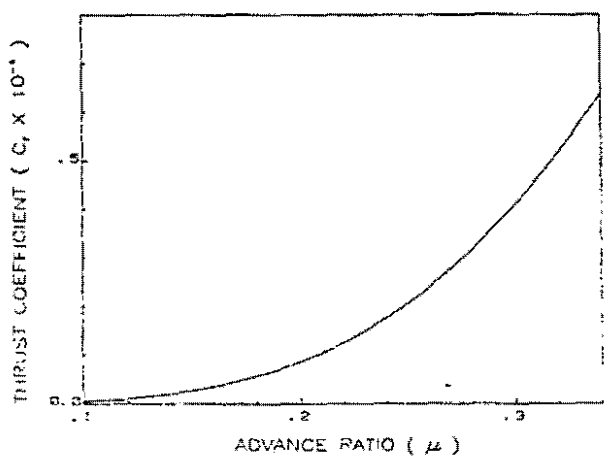


Figure 5 Variation of $C_T$ with Advance Ratio

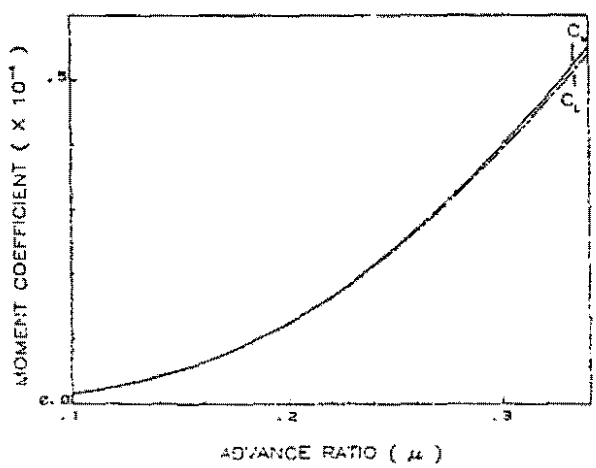


Figure 6 Variation of $C_M$ and $C_L$ with Advance Ratio

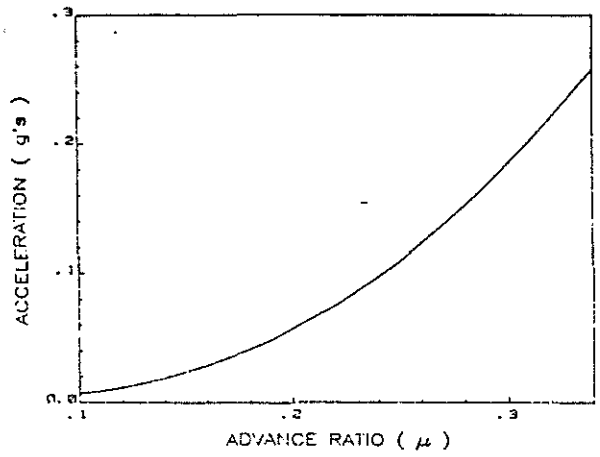


Figure 7 Variation of Acceleration at the Pilot Seat with Advance Ratio— Finite Element Model

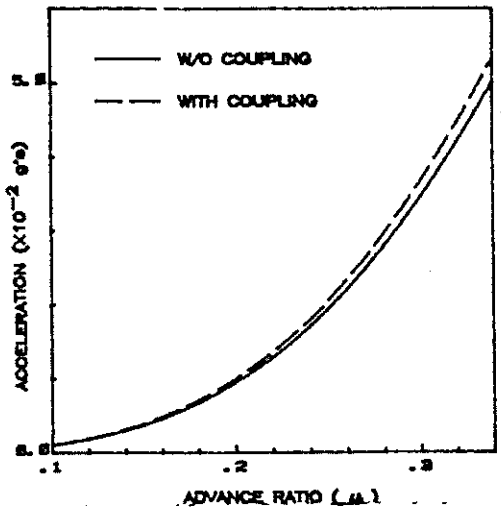


Figure 7a Variation of Acceleration at the Pilot Seat with Advance Ratio— Assumed Mode Model

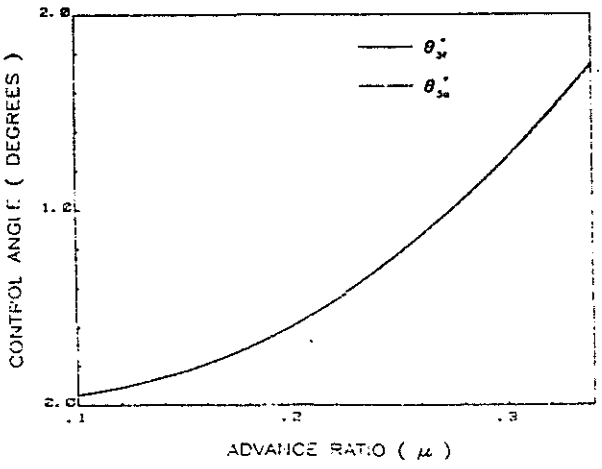


Figure 8 Comparison of Control Angle $\theta_3$ from Minimization of Forces and Accelerations — Finite Element Model

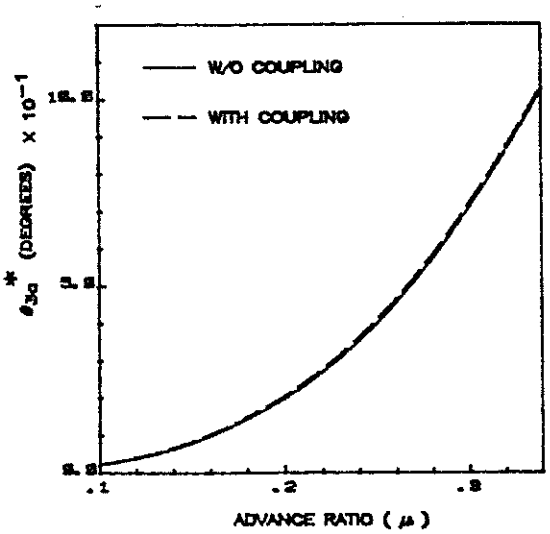


Figure 8a Comparison of Control Angle $\theta_3$ from Minimization of Accelerations with and without Coupling — Assumed Mode Model

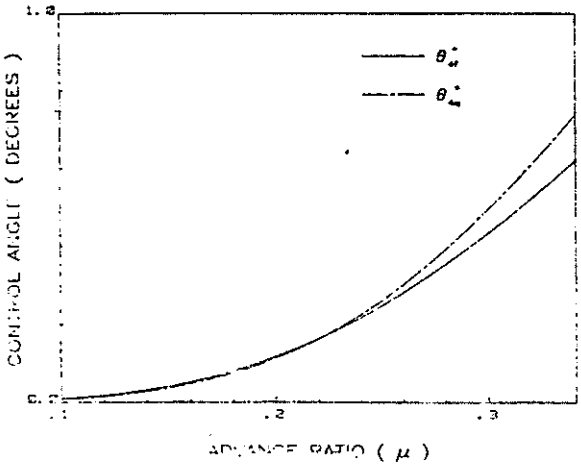


Figure 9 Comparison of Control Angle $\theta_4$ from Minimization of Forces and Accelerations — Finite Element Model

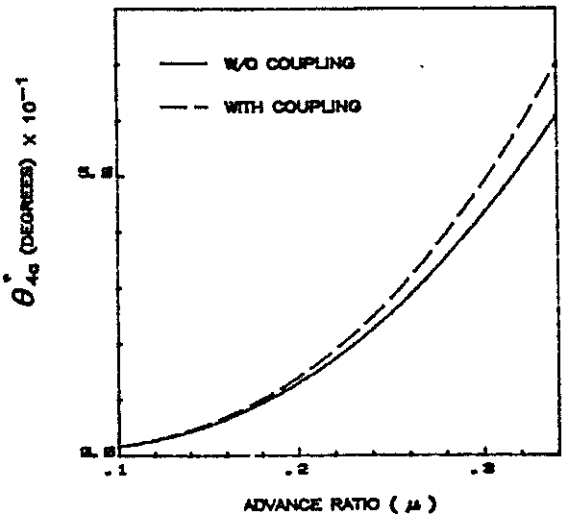


Figure 9a Comparison of Control Angle $\theta_4$ from Minimization of Accelerations with and without Coupling — Assumed Mode Model

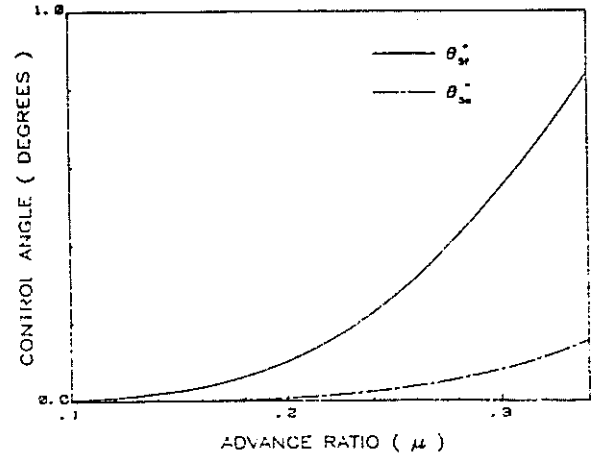


Figure 10 Comparison of Control Angle $\theta_5$ from Minimization of Forces and Accelerations — Finite Element Model

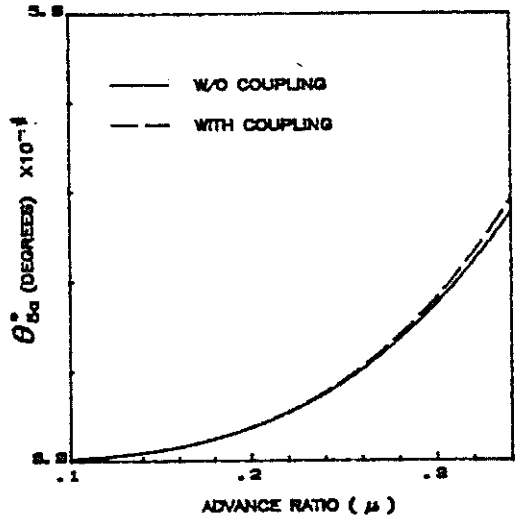


Figure 10a Comparison of Control Angle $\theta_5$ from Minimization of Accelerations with and without Coupling — Assumed Mode Model

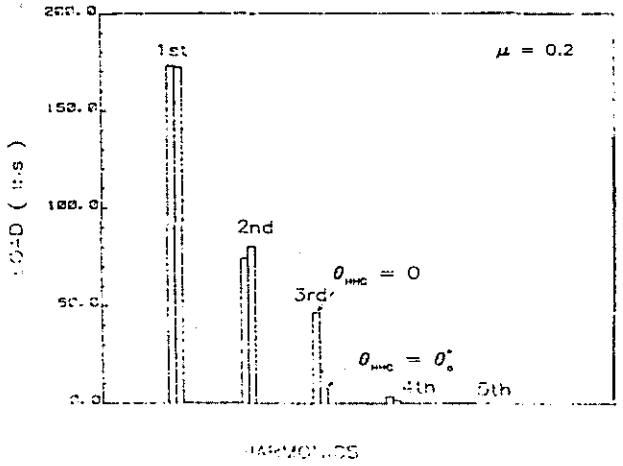


Figure 11 Harmonics of Blade Shear Force at Root

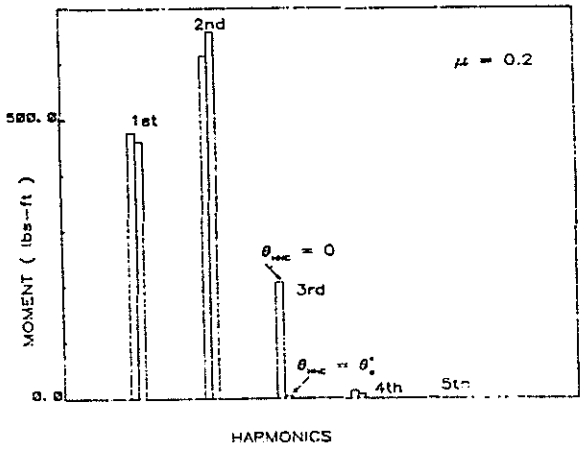


Figure 12 Harmonics of Blade Bending Moment at Root

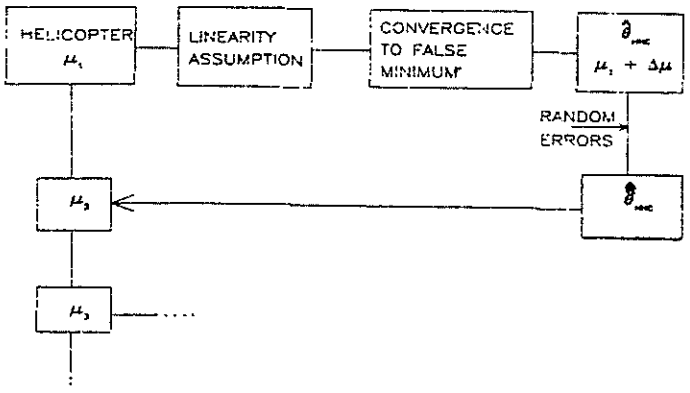


Figure 13 An Error Model for HHC

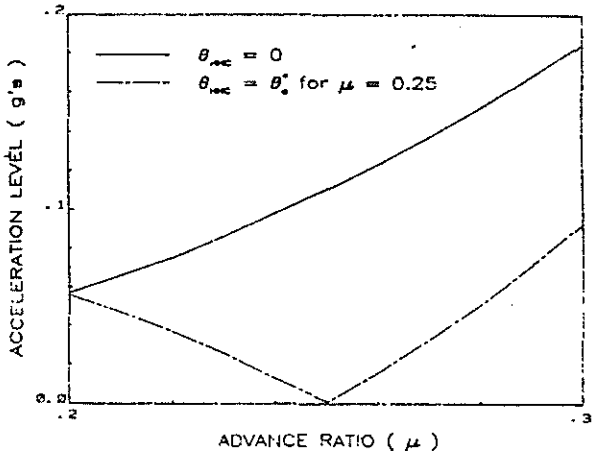


Figure 14 Acceleration at the Pilot Seat with Incorrect Advance Ratio

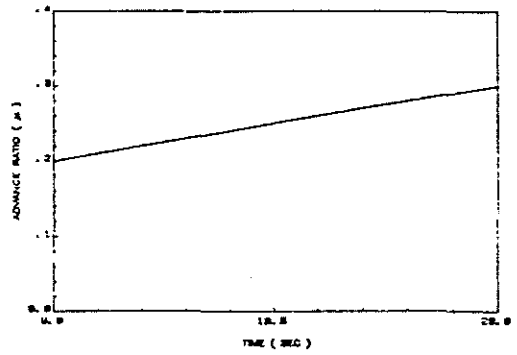

Figure 15 Variation of Advance Ratio with Time

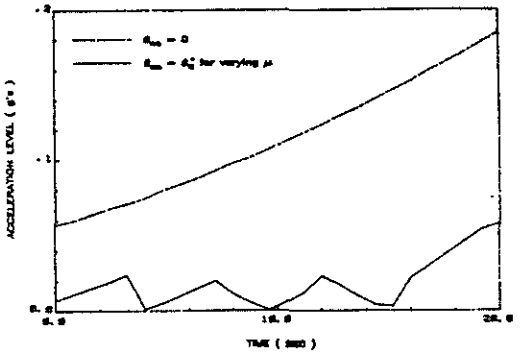

Figure 16 Accelerations Due to Discrete Time Control